Geophysical and Geodetical Investigation of A Landslide Area (Koyulhisar-Sivas, Turkey)

Sevda Özel[1], Demet Över[2], Kemal Ö. Hastaoğlu[3]

[1,2]Department of Geophysical Engineering, Cumhuriyet University, 58140, Sivas, Turkey
[3]Department of Geomatics Engineering, Cumhuriyet University, 58140, Sivas, Turkey

Correspondence to: Sevda Özel (sozel@cumhuriyet.edu.tr.)

Abstract. The study area is in the last section in the close south of Koyulhisar (Sivas) landslide site and the study area is in the most active location where the landslide's displacement amount is the highest. The landslide site was examined with geophysical (SRT-seismic refraction tomography, GPR-ground penetrating radar) and geodesic (GNSS-global navigation satellite system) methods. According to the geophysical results, within ~20 m of investigation depth, three layers with the average seismic P-wave velocities (V_P) of 0.30, 1.00 and 2.00 km/s have been identified. It was determined that the thickness of the first two layers of these layers from top to the bottom is approximately 3 and 6.5 m, and the last layer with Vp>2.0 km/s is the bedrock. Furthermore, in geophysical sections, it was determined that the depth of the sliding surface which is the upper limit of the bedrock varies between ~7-10 m. The geophysical results permitted to identify the landslide type as planar sliding, with the sliding direction in S-SE, and the tilt of the layer being orientated in the same direction as the topography slope (mostly bigger than 5°). In addition, according to geophysics and geodetical results, it was observed that the deformations in the landslide mass have occurred from the geological unit, the layer or topography slope, and precipitation. Therefore, it was thought that landslide activity may continue in the study area. These results were showed that precipitation and deformations within the layer can be effective in triggering the landslide in the future. Therefore, the study area contains the risk and the natural hazards, and these threaten the settlement area and the buildings and other constructions there.

1 Introduction

A landslide is a mass movement and can occur in the different forms. Koyulhisar landslide area, the subject of this article, is one of the largest landslide areas that significantly lead to serious loss of lives and property as in throughout Turkey. Three of the most destructive of these landslides occurred in Koyulhisar (Sivas) on 19 August 1998, 20 July 2000 and 17 March 2005. The Koyulhisar landslide area is one of the most important large landslide areas in the country and mass movements there typically occurs in the form of debris or mudflow (Tatar et al., 2007; Duman et al., 2005). In addition, Koyulhisar is an active landslide area and for the past 17 years, there has been observed an increase in landslide activity (Tatar et al., 2007; Över, 2015). The large and small landslides in Koyulhisar landslide area have mostly occurred due to natural causes until today. Artificial causes mainly constitute the landslides caused by human interventions (blasting, drilling, improper planting, loading, loss of vegetation cover, etc.). The last large landslide occurred with the flow of mud in the north of Koyulhisar landslide area in March 2005. Duman et al. (2005) determined that this landslide was in the excessively fast (6 m/sec) class. Demirel vd. (2016), for the landslide in 2000 year revealed an average of 2.5-7.4 mm/year slip rate. In addition, researchers have stated that these landslides usually have a mechanism involving a circular rotation, this old landslide mass maintains its activity and partial landslides occur on the groundmass (Sendir and Yılmaz, 2001; Duman et al., 2005). Therefore, Koyulhisar district center is on an old landslide that occurred in the form of circular rotation. The front of this landslide mass is open, it is always active, activity is not massive and usually in the form of local landslides occurring on the groundmass (Sendir and Yılmaz, 2001).

The triggering mechanisms of landslides are often complex and further understanding is needed to facilitate the prediction of mobilizations as well as adequate stabilization and remediation measures. Therefore, it is important to investigate the reasons that affect the formation mechanisms and the formation of landslides. Different engineering (geology, geophysics, geodetic, etc.) disciplines have great role and importance especially in decreasing the landslide effects. They can help to prevent damage by prediction and early warning. In this context, Koyulhisar landslide area was examined in a wide area with detailed GNSS (Global Navigation Satellite System) methods and the studies of other disciplines (geology, chemistry, seismology, meteorology, remote sensing) (Sendir and Yılmaz, 2002; Tatar et al., 2007; Hatiboğlu, 2009; Hastaoğlu and Şanlı, 2011; Yılmaz, 2009; Hastaoğlu, 2013; Türk, 2013; Topal and Hatiboğlu, 2015; Hastaoğlu, 2016). The annual sliding velocity, sliding direction, displacement amounts and natural disaster risk of the landslide have been identified by these studies. It has been determined that the displacement amounts of the landslide velocity vary between 1-8.6 cm/year by topography and geological bedding and that the landslide direction is usually S-SE oriented. In terms of geology, some researchers have carried out geological studies on many issues such as geological, tectonic, geotechnical, geochemical and geomorphological studies at the local and regional scale in which the features of the faults, water, hot water, soil and rock on the NAFZ (North Anatolian Fault Zone) and in the region were investigated. These studies are in geology, tectonics (Toprak, 1989; Uysal, 1995; Sendir and Yılmaz, 2001; Sendir and Yılmaz, 2002; Yılmaz et al., 2005; Gökçeoğlu et al., 2005b; Demirel et al., 2016; Demir, 2018), and geotechnics, geomatics/remote sensing, geochemistry and geomorphology (Toprak, 1989; Uysal, 1995; Duman et al., 2005; Ulusay et al., 2007; Hatiboğlu, 2009; Yılmaz, 2009; Demirel et al., 2016; Demir, 2018). The results of all these studies have been associated with geophysical results at the interpretation stage in this article and the geophysical studies were carried out for a limited area being the subject of this article and had the distinction of being the first geophysical studies.

In the geophysical study, the hazards that would be caused by the landslide geometry of the last section in the close south of Koyulhisar landslide area and would affect the settlement area were investigated (Fig. 2 and 9). The geophysical study was also carried out in this area which is the most active area of the landslide site because Hatipoğlu (2009) identified a movement of about 8.6 cm/year in this area. The SRT (Seismic Refraction Tomography) method determining the seismic P-wave velocities (V_P) for seismic applications and the GPR (Ground Penetrating Radar) method for electromagnetic (EM) applications were used in the geophysical data collection in the area. In particular, seismic tomography (SRT, MASW) and ground penetrating radar (GPR) applications are preferred methods in landslide studies. The structural geometry of the landslide area was delineated based on an interpretation of the collected geophysical data. These are the seismic V_P velocities, thickness, tilt and direction of the layers. Thus, other features such as the sliding surface depth of the landslide, landslide type, advancement direction and the risk situation were also revealed, and geophysical and other study results were shown to be compatible with each other. The studies carried out by McCann and Forster (1990), Demirağ (1991), Hack (2000), Perrone et al. (2004), Göktürkler et al. (2008), Hu and Shan (2016), Su et al. (2016) and (Popescu et al. 2016) are important in this regard. In addition, Bichler et al. (2004) carried out multi-methodical geophysical studies containing electrical resistivity, GPR and seismic methods in the landslide studies. Otto and Sass (2006) and Ristic et al. (2012) also carried out similar studies on landslide investigation.

In these studies, the sliding surface of the landslides and the flow direction properties of the landslide material were generally determined by 2D (two-dimension) and 3D (three-dimension) geophysical sections.

It has been observed that the use of the SRT and GPR methods in landslide studies has increased significantly especially in recent years (Ristić et al., 2012; Timothy et al., 2013; Lissak et al., 2015; Hu and Shan, 2016; Popescu et al., 2016; Su et al., 2016). The parameters which define the landslide such as landslide geometries and bedrock depth or sliding surface depth have been determined in these studies. Regarding the GPR method, significant studies have been carried out by Davis and Annan (1989) on revealing the soil stratigraphy, by Aldaş et al. (2003), Slater and Niemi (2003) and Green et al. (2003) on the mapping of faults, fractures and cracks and by Benson (1995), Harari (1996), Bano et al. (2000) and Bubeck et al. (2015) on the determination of groundwater levels. However, the accurate determination of the landslide type is also very important as well as landslide elements. Joint studies with geophysics and other disciplines are commonly carried out in determining the landslide type and for different contributions. In addition to these, the seismological history, morphological and topographical features and meteorological data of the study area are always taken into account in the landslide analysis. They are largely used in such studies especially for their contribution to interpretation. In this article, the information obtained from all these data was used in order to make contributions to the geophysical results. For, landslides may develop under various geological, morphological, topographical and physical reasons. Thus, through multi-discipline studies, the landslide type can be determined most accurately by determining different sliding behaviors (such as the velocity and direction of the landslide, annual amount of displacement) varying from region to region. The landslides, which generally occur in the form of sliding, may occur with the movements of falling, sliding and flowing or with the combination of a few of these. Therefore, accurate determination of the landslide type/kind and the selection of the methods used in the study is very important. It may be possible to perform an accurate landslide analysis only if these requirements are met. In this article, these issues were examined and discussed separately and together with geophysical and geodetic results.

2 Geology

The study area is about 180 km away from Sivas city center and is in the west of Koyulhisar district center which is located in the north of the NAFZ (Fig. 1 and 9). The rocks in the region usually have fractures and discontinuities and are crushed because of the NAFZ which is tectonically active in south of the study area (Tatar et al., 2005). There are also many old and new landslides in the study area depending on the high tilted topography. For these reasons, the directions of movement of the landslides generally threaten the settlement areas (Sendir and Yılmaz, 2001). The geological investigation of Koyulhisar has been carried out regionally or locally by various researchers (Terlemez and Yılmaz, 1980; Toprak, 1989; Uysal, 1995; Sendir and Yılmaz, 2002; Duman et al., 2005; Hatiboğlu, 2009). According to these studies, the Plio-Quaternary aged Koyulhisar Formation is the youngest unit in the region. It was stated that the youngest unit consisted of the talus (slope or deposit) and fluvial conglomerates and was seen along the strike-slip faults (Toprak, 1989).

Toprak (1989) divided the NAFZ which is represented by a right lateral strike-slip fault zone into five fault sets including the North Anatolian Main Fault, Koyulhisar fault sets, Kelkit fault set, Şıhlar fault set and Kuruçay fault set. But, the Şıhlar fault sets affect Koyulhisar district center at the nearest (Fig. 1). Toprak (1989) stated that Koyulhisar section of the NAFZ is still active and a right lateral strike-slip fault zone due to the morphotectonic structures and seismic activities in the region (Fig. 1). As it is seen in Fig. 1, the faults closely concerning Koyulhisar are the NAFZ, which is the main fault extending in the northwest-southeast direction and approximately 2-2.5 km away, in the south, and the Çamlıyaka Fault, which is approximately north-south-oriented, in the west. This fault which is the closest one to the study area extends perpendicular to the NAFZ in the south. It was also reported by Tatar et al. (2007) that large and old landslide masses in Koyulhisar landslide area have lower Miocene-aged clay and gypsum levels, Eocene-aged clayey levels and Plio-Quaternary aged sediments. However, Hatiboğlu (2009) and Hastaoğlu et al. (2015) generally observed two geological units in the drillings in the study area. They observed that the upper unit was silty sandy clay and sand interbedded silty clay in some places up to about 10 m, and advanced as sand interbedded silty clay and sand interbedded clay in some places towards deeper than 10 m. The first unit consists of light-dark brown colored, medium-very stiff, low-high plasticity, silty clay. The second unit consists of light-yellow white colored, low-high plasticity, silty sandy clay interbedded with sand (Hastaoğlu et al., 2015). When the drilling logs are examined, there is generally the second unit in east of study area (Hastaoğlu et al., 2015). Furthermore, it was observed that the content of the second geological unit did not change even if the depth of the drilling increased. Therefore, the second geological unit was taken into consideration in the interpretation of geophysical sections.

3 Methods

3.1 Geophysical surveys

The SRT and GPR methods which are applied in tomography format were used in the geophysical study. The high-frequency electromagnetic waves can reach deeper in the environments with low conductivity like sand. However, the conductive units such as clay and shale decrease the penetration depth of the signal transmitted and lead to absorption (Annan et al., 1988; Davis and Annan, 1989). Firstly, SRT and GPR data were collected along multiple transects in two different areas of the study area named A and C (see Fig. 2). Then, the geophysical profiles were processed to the satellite map according to the coordinates along with the topographical elevation curves and GNSS measurement locations for the ease of interpretation (Fig. 2a). Geophysical measurements were taken as both NE-SW and NW-SE oriented due to the geologic bedding and topographic features (Fig. 2b-c). However, SRT12-GPR12 profiles were selected as about E-W oriented due to rugged topography in area C. The profile lengths usually range from 40 to 60 m according to the method applied. The profile shooting technique in the field, hammer and iron plate of 8 kg weight as the source P geophone of 14 Hz (the total number of geophones is 12) and Geometrics branded seismic device as the receiver Geometrics branded seismic device as the receiver was used while collecting the SRT data. In all profiles, the geophone interval was 5 m, offset distance was 2.5 m, sampling interval was 256 ms and the record length was 512 ms. The geophones were respectively fixed on the ground within the selected geophone range and their connections with the seismic device were made. Then, seismic measurements were recorded by starting from the offset distance of 2.5 m, reducing to sledgehammer plate and making at least 5 times shots between each geophone, respectively. In the evaluation of the SRT data collected in the field, SeisImager program was used for displaying, processing and evaluation of the seismic refraction waves. The marking of the first arrivals of the SRT data was performed using Pickwin, and the evaluation of the first arrival data was performed using Plotrefa module.

The GPR data collected on the SRT profiles only in the areas A and C were collected by Ramac2 device using a closed antenna of 250 MHz. The GPR data were processed in Reflexw program. In order to collect the GPR data, other parameters were selected 512 ns-number of samples, 16-number of stacking and 0.1 m-trace interval. 2D GPR data processing, it includes Static correction, Muting, Bandpass filter, Gain and Migration steps. The migration was made to show up small vertical structures invisible during data processing. Thus, very large hyperballs with strong reflections may limit the display of non-migrated GPR data. Moreover, the peak points of hyperbolas observed in GPR cross-sections show the reflection surface of the electromagnetic wave. During data processing, velocity analysis was performed on the reflection surfaces through the hyperbola superposition method and EM wave propagation velocity was calculated in all GPR cross sections. The topographic corrections were made by selecting the “Correct for two layers” option in Static Correction/Muting in the Reflex program. The height values collected in the study area were manually entered and saved in “Correct for two layers” option. Thus, the models were converted from m to ns and the GPR sections were prepared for interpretation.

SRT profiles and on these seismic profiles GPR profiles in the area defined by A in Fig. 2b are approximately in the NE-SW (SRT2, SRT4, GPR2, GPR4)) and NW-SE (SRT3, SRT5, GPR3, GPR5) directions (Fig. 2b). In area C and in the west of this area, SRT10-SRT11 profiles and on these profiles GPR10-GPR11 profiles are approximately in the E-W directions. In the same area, SRT9-SRT14 profiles and on these profiles GPR9-GPR14 profiles are approximately in the NE-SW direction (Fig. 2c). Similiarly, in the east in Fig. 2c, SRT12-GPR12 profiles are in the E-W directions and SRT13-GPR13 profiles are approximately in the NE-SW directions. In addition, geomorphologically the landslide cracks on the surface, displacement traces, and structural damages in the study area and its immediate surroundings can be monitored clearly by field observations and visibly the damaging effects of still active or old landslides on residences, roads, walls can easily be observed (Fig. 3). All damaged structures across the region cannot be used. Therefore, new landslide cracks will emerge over time both on the ground and the existing structures in the region which active in terms of landslide and seismicity, and the formation of new landslides will continue in the area.

3.2 Results and interpretation

The time-depth sections which were ready for interpretation were obtained by increasing the signal/noise ratios of the signals in the data processing. The geophysical sections were prepared by also making a topographic correction in the inversion operation due to the variability of the topography. Thus, the collected geophysical data were converted into 2D (two-dimension) height-distance and depth-distance sections by being assessed in the appropriate software. Geophysical interpretations were made according to these sections and compared with the results of the other studies.

SRT: 2D (two-dimension) seismic cross-sections giving seismic V_P-depth information are presented in Fig. 4 and 5. In the seismic data evaluation, the coincidence was provided with RMS (Root Mean Square) errors ranging between 3.4-4.5% in 2D (two-dimension) inversion operation. According to 2D (two-dimension) seismic cross-sections, two or three layers were identified at about 20 m depth. It was understood that the tilts of these layers were southeast oriented, and their tilt was greater than 50^0. According to seismic velocities (V_P) calculated, three layers with the layer velocities of 0.30, 1.00 and 2.00 km/s on average were defined from top to bottom. V_P values of these layers increase towards the deep. Layer thicknesses range between 3 m and 6.5 m on average from top to bottom due to topographical differences. It was understood that the depth of the sliding surface varied between about 7-10 m, and these depths were the upper bound of the third layer. This area was considered to have a risk of dislocation due to these loose units, rainfall and tilt conditions. Therefore, the layers with an average of V_{P1}=0.3 km/s and V_{P2}=1.00 km/s over these depths were defined as the layers with the risk of dislocation. The layer with a seismic velocity of greater than V_{P3}>2.00 km/s at the lowermost was understood to be the basement layer. The investigation depth was further calculated from the SRT sections compared to the GPR sections due to the differences of geophysical methods in the application. Because GPR sections were obtained in well-resolution for about the first 10 m depth after inversion processing of the GPR data (Fig. 6 and 7). Therefore, it could be said that the GPR and SRT sections are compatible for the first 10 m depth. Besides, the profile lengths of the GPR3 and GPR5 sections in Fig. 7 were evaluated as about 25-35 m.

GPR: The GPR sections, it was obtained in high-resolution for about the first 10 m depth. It is clearly observed that the strong reflections are within 10 m depth in Fig. 6 and 7. These strong reflections seen in black dashed ellipses are interpreted as deformation areas in the layer. In a similar manner, these areas being interpreted as deformations were also observed in the studies of Bubeck et al. (2015), Hu and Shan (2016), Su et al. (2016) and Popescu et al. (2016). The strong reflected wave signal shows distinctive characteristics, presenting a low-frequency high-amplitude sync-phase axis, which can be inferred as the sliding surface in Fig. 6 and 7. Furthermore, in Fig. 6 and 7, there is a layer with a varying thickness of about 3 mm at the uppermost. It is seen that the second layer under this layer proceeds until about 7-10 m depth. In other words, two layers were identified in GPR sections. These layers are weak, loose, cracked, moved and also have lost their tightness, and their seismic velocities are low. Therefore, in Fig. 6 and 7, it was thought that deformations developed on the sliding surfaces due to the geology of the study area in A and C area. Because the first geological unit is medium-very stiff, low-high plasticity, silty sandy clay. The deformation structures as sliding surfaces, landslide furrows, scarps, collapsed zones, and cracks were observed in the GPR cross-sections (Fig. 6 and 7). However, three layers were identified in seismic sections, and their seismic velocity was observed to increase towards the depth (0.30<1.00<2.00<… km/s). Accordingly, in GPR sections, the fact that the problems seen in the first two layers decreased and ended towards deeper layers (>7-10 m) is understood from the increase in seismic velocities (>2.00 km/s). Furthermore, the electromagnetic wave velocity in the GPR sections was calculated. In Fig. 8, the EM wave velocity calculated for the reflection surface in GPR5 cross-section -representing the GPR profiles- was shown as an example. The picks were exported with the attribute of two-way travel time, and the velocity of propagation of the wave, in this case, appears to be about 0.1 m/ns (Fig. 8). This value is generally observed in dry or wet soil, dry or wet clay and sandy environments (Wilchek, 2000; Cardomina, 2002). Therefore, it was thought that this velocity value was compatible with the geological units and electromagnetic waves led to rapid absorption due to the silty sandy clay layer. In other words, the geological unit, the layer or topography slope and precipitation cause deformations in the loose upper unit. Therefore, these structures may develop or occur in the landslide mass, as shown in Fig. 6 and 7.

3.3 Seismological and meteorological data and results

The study area is located in an active area in terms of seismicity. The seismological history, the magnitude (M) of which is greater than 2.5, of the examined area and its surrounding between 1900-2015 were investigated for this article (Fig. 9). The map in Fig. 9 was prepared with the seismological data between 1900-2015 (UDİM, 2016). Particular attention was paid to the earthquakes before 2005 in the seismological interpretation. This is because the largest and most recent landslide occurred in the area in 2005 and it was aimed to investigate its relationship with displacements and previous landslides. The type of magnitude which is calculated from seismological data is usually the local magnitude. The depths (d) of these earthquakes with higher M>2.5 vary between approximately 5 and 80 km (Fig. 9). According to the seismic data of the years examined, Koyulhisar and its surroundings have always been active seismically. It was observed that this frequency of earthquakes usually occurred on the NAFZ in the south of the study area. Additionally, it has been analyzed the seismic activity of the region at least for the last 112 (1904-2016) years by Demir (2018). In this study, he express that the most notable is probably the relationships between the magnitude of the earthquake to the number of landslides and the area affected by the landslides and between the magnitude and the maximum distance of landslide observations from the epicenter in different geological, topographical, and climatic conditions (Demir, 2018).

Large earthquakes affecting Koyulhisar district also occurred in the region. These largest earthquakes are in the south of the NAFZ or Suşehri district and a total of three large earthquakes with M≥5.6 occurred there (Över, 2015). Among these, 1992 earthquake is closest to the study area with the least depth but the second largest earthquake (Fig. 9). This earthquake is an earthquake with 6.1 magnitude that occurred 10 km below the ground. The large earthquakes in the south of Suşehri district which is just 13 km away from the study area occurred in 1909 and 1939. 1909 earthquake occurred 60 km below the ground and is the largest and deepest earthquake with a magnitude of 6.3. 1939 earthquake is also deep and the third largest earthquake that occurred 50 km below the ground with a magnitude of 5.6 (Över, 2015). In addition, when Fig. 8 is analyzed, it is seen that the magnitudes of the other earthquakes in the north of the NAFZ and the upper elevations of the landslide generally vary between 2.5-4. Similarly, it is seen that the other earthquakes in the south of the landslide area are the earthquakes with a magnitude of greater than 3.6. All these earthquakes may have triggered the landslide mass from time to time in places where sliding surfaces, layers, and topography in the landslide area are more inclined than 5-10 degrees (according to the geophysical cross-sections in this article, when it is considered that there are loose units and deformations on the sliding surfaces). In particular, they further affected the landslide mass along with the rain and caused large amounts of displacement in the landslide area.

The data regarding the rainfalls with the effects of triggering the landslides are presented in Table 1 and Fig. 10 (MGM, 2016). With these data, the rainfall status of the study area and its surrounding was examined by months as average annual rainfalls and the annual areal amount of rainfall. According to the data obtained between 1950-2015 in Table 1, the rainy periods are generally between October-November-December and January-February-March-April. The highest total daily amount of rainfall in the rainiest years was observed as snowfall in 1950 (110 cm) and as rain in 1991 (55 kg/m^2).

According to Fig. 10, the annual normal average rainfall value calculated for the years between 1981-2010 was calculated as over 483.4 mm. However, 1987-1988 and 1997-1998 were the rainiest years. It is seen that the annual areal amount of rainfall exceeded the normal values and was higher than 550 mm in these rainy years that took place in every 10 years. Similarly, it is also seen that there were high rainfalls for 3-4 years after the years of 1985-1995-2005 with an interval of 10 years. Therefore, annual areal rainfalls were observed to be more before some large landslides like the landslide in 1998. When geological features of the region are taken into account, it is remarkable that the landslide in 1998 and 2000 occurred in the summer months after the winter with a heavy fall of snow. However, the landslide in 2005 occurred during the rainy season. Therefore, rainfalls have always been considered as a factor triggering these landslides in many studies and articles (Tatar et al., 2007; Hastaoğlu et al., 2015). Similarly, the authors of this article have always considered rainfalls as a triggering factor in the formation of Koyulhisar landslides. As it is seen, the various studies and the results of this article have proved that Koyulhisar landslides are generally caused by the known reasons that trigger the landslide. Therefore, these conditions mentioned in the landslide area have shown that the landslides could be triggered there.

3.4 Geodetic surveys and results

GNSS studies and multi-disciplinary studies have carried out for many years (about 6 years) to determine the deformation and annual sliding amounts especially after the landslides in 1998-2000-2005 (Hastaoğlu et al., 2015). It was determined that the tension cracks that occurred in the landslides in 1998 and 2000 in the region were filled with the waters consisting of melting snow and rain waters which are the most important component of the hydrological cycle, lakes were formed in the buttress of each sliding mass, and the changes in the groundwater level were the main causes of deformation (Sendir and Yılmaz, 2001; Topal and Hatiboğlu, 2015; Hastaoğlu et al., 2015). The seismological and meteorological data, which were updated by the geodetic (GNSS (DH), geological (IDH (Inclinometer Drilling Holes)) and meteorological data collected in the local study of Hastaoğlu et al. (2015), were reorganized and evaluated. Fig. 2, 10, 11 and Table 1 which were reprepared for the study which is the subject of this article were associated with the results of GNSS studies (studies made by Hastaoğlu et al. (2015)) (Fig. 11). Then, they were compared with geophysical results in interpretation.

The monthly and annual meteorological data should certainly be evaluated particularly within the scope of monitoring activities because the area which is the subject of the study is a landslide area. Hastaoğlu et al. (2015) performed monitoring in IDH wells in the area in 2013-2014 (Fig. 11). If Fig. 2 is examined, there are seven IDH point in the nearest of the geophysical profiles. The graphics in Fig. 11 were prepared from the combined data (unpublished data in the project) and the temperature (^{0}C), precipitation (m^3) and soil moisture content (cm) were compared in these graphics. Accordingly, the temperature and precipitation were observed to be inversely proportional during the summer months called as a dry period. It is seen that the soil moisture is changeable apart from the rainy period and has very high water content during the rainy periods. The soil moisture is very high (average 150 cm) in winter, summer, autumn seasons (Fig. 11). In study area, the water contents in the drilling data change from 24.6 % to 13.3 % at between 0-10 m depth and these values are also high (from 29.1 % to 17.3 %) after 10 m (Hastaoğlu et al., 2015). Water generated from precipitation, melting snow and permafrost melting is blocked by the impermeable layer when it infiltrates downward, and the local moisture content increases (see Hu and Shan (2016)). Thus, the water infiltrates the interface between the permeable and impermeable layer, can form a slip zone. The GPR results show that the moisture content of soils at the sliding surface of the landslide mass is relatively high. The drilling data and soil moisture values also show very high moisture content of the sliding surface of the landslide mass in the study area, which is completely consistent with the results obtained from the GPR-SRT profiles, meteorological and geological results. On the other hand, it was understood that the precipitation increased by the decrease in temperatures. It is also seen that the total annual amount of rainfall increased about 2-fold in 2014 compared to 2013 (Fig. 10 and 11). According to all results, rainfalls are considered to be effective in triggering of the landslide because the ground of this landslide area, which is filled with loose units and old cracks, is supersaturated with water due to the rainfalls.

Besides, Hastaoğlu et al. (2015) determined that the groundwater level gets close to the surface for 4-6 m on average at the end of the rainy period, to 10 m at the end of the rainy period and decreases up to 25 m in some wells in the area where geophysical study area is also located, and the groundwater flow direction is SW. When this information was associated with topography and in line with the field observations, it was understood that the topography was inclined from the north of the study area towards south, the incline of slope decreased from

925 m to 840 m, there was an elevation difference of 85 m, and the amount of slope in the topography increased from south to north (>5^0-10^0) (Fig. 2a). Therefore, it was seen that the geological bedding was compatible with the topographical sloping and the groundwater was compatible with the direction of flow. The geological units were observed in IDH wells in the geophysics study area. These are mostly silty sandy clay and they have different characteristics above and below about 10 m in IDH well. Hastaoğlu et al. (2015) estimated with the GPS measurements that the amounts of displacement varied between 1-8.6 cm/year. The geophysical data were collected in the areas where the amount of displacement varied about 8.6 cm/year. The landslide direction was determined to be in the S-SW and SE direction across Koyulhisar (Hastaoğlu et al., 2015). It was understood that these directions were compatible with the geophysical sections which were prepared later and that the rainfalls are among the reasons that trigger the landslide.

4 Conclusions

This study is the first geophysical study carried out in Koyulhisar landslide area. The information provided from many studies (geodetic, geologic, morphologic, seismological, topographic and meteorological) carried out across the region was compared with the geophysical results (SRT and GPR) and found to be compatible. The bedding status of the landslide area, seismic P-wave velocity (V_P) of the layers, the tilt, tilt direction of the layers, depth of the sliding surface and sliding direction and the landslide type could be determined from the geophysical sections. Accordingly, the study area was identified by the layers with the average seismic velocities of 0.30 < 1.00 < 2.00 <… km/s (or 300, 1000 and 2000 m/sec). The seismic velocity of the landslide basement was found to be higher than 2000 m/sec. According to the geophysical cross-sections, it was identified that the depth of the sliding surface varied between 7-10 m due to the topographical differences. These depths are the depths with low seismic velocities (the average V_P, <0.30 and <1.00 km/s) and defined as loose units which were also observed in geological drilling logs. It is determined that sliding surfaces, landslide furrows, collapsed zones, scarps, cracks are observed in the GPR sections. Furthermore, it was understood that the layer tilt was generally more than 5^0 in all geophysical sections and compatible with the geology and the flow direction of the groundwater. It was understood that the landslide type in the area was planar sliding and the direction of sliding was SE.

The geophysical and geodetic study results were found to be compatible because it is known that the landslide direction across Koyulhisar is in S-SW and SE. Consequently, the fact that the depth of the sliding surface over the units is loose, low seismic velocities of the upper layers and the excessive tilt show that there is a new risk of landslide in the area. The other factors that trigger the landslide were found to be associated especially with the fact that the area is seismically active, receives heavy rain and has a poor vegetation cover. Furthermore, it was understood that there were deformations in the landslide mass and, observed the sliding surfaces, landslide furrows, collapsed zones, scarps and cracks structures. It was understood that these structures were occurred from the geological unit, the layer or topography slope, and precipitation. On the other hand, it was thought that studies such as blasting and excavation performed by human intervention can trigger the landslides due to the geologically loose unit and hence the landslide area can a potential area which is open to natural/artificial hazards. As a result, according to all the results, there is still a high landslide hazard in the study area and its surrounding, and this hazard will be also in the future. As a result, the identified risks and natural hazards are also threatened the settlement area and the buildings and other constructions (e.g. roads, walls, parks et al.) there. Therefore, it was understood from the geophysical and geological data obtained for the landslide basement and the layer over it that new landslides may occur over time in the study area due to the tilt and abrasion and transports during precipitation.

Acknowledgments: This study was supported by Cumhuriyet University Scientific Research Projects Commission as CÜBAP Project numbered M-464. We would like to thank Project Coordinator Assoc. Dr. Kemal Özgür Hastaoğlu and his research team, who allowed us to benefit from the results of TÜBİTAK supported project numbered 111Y111, for their contributions. We would like to thank Dr. Çağrı Çaylak for his contributions during the geophysical field measurements, Assoc. Dr. Fatih Poyraz for his contributions during the process of geodetic field measurements and Assoc. Dr. Tarık Türk. We would like to thank Geological Engineer Mehmet Demirel for his contributions to the Fig. 2.

References

Adlaş, G. U., Kadıoğlu, S., Ulugergerli, E. U.: The effects of concealed discontinuities in blast design Pattern, 4th Int. Scientific and Technical Conference of Young Scientists and Specialists, St. Petersburg-RUSSIA, 6-7, 2003.

Annan, A. P., Davis, J.L., Gendzwill, D.: Radar Sounding in Potash Mines: Saskatchewan, Canada. Geophysics, 53, 1556-1564, 1988.

Bano, M., Marquis, G., Niviere, B., Maurin, J. C., Cushing, M.: Investigating alluvial and tectonic features with ground penetrating radar and analyzing differactions paterns, J. Appl. Geophys., 43, 3-41, 2000.

Benson, A. K.: Applications of ground penetrating radar in assessing some geological hazards: Examples of groundwater contaminants, faults, cavities, J. Appl. Geophys., 33, 177-193, https://doi.org/10.1016/0926-9851(95)90040-3, 1995.

Bichler, A., Bobrowsky, P., Best, M, Douma, M., Hunter, J., Calvert, T., Burns, R.: Three-dimensional mapping of a landslide using a multi-geophysical approach: the Quesnel Forks landslide, Landslides, 1, 29-40, DOI 10.1007/s10346-003-0008-7, 2004.

Bubeck, A., Wilkinson, M., Roberts, G. P., Cowie, P. A., McCaffrey, K. J. W., Phillips, R., Sammonds, P.: The tectonic geomorphology of bedrock scarps on active normal faults in the Italian Apenninesmapped using combined ground penetrating radar and terrestrial laser scanning, Geomorphology, 237, 38-51, DOI:10.1016/j.geomorph.2014.03.011, 2015.

Cardimona, S.: Subsurface investigation using ground penetrating radar, Presented at the 2nd International Conference on the Application of Geophysics and NDT Methodologies Transportation Facilities and Infrastructure, LosAngels, California, 2002.

Davis, J. L., Annan, A. P.: Ground-penetrating radar for high resolution mapping of soil and rock stratigraphy, Geophys. Prosp., 37, 531-551, DOI: 10.1111/j.1365-2478.1989.tb02221.x, 1989.

Demir, G.: Landslide susceptibility mapping by using statistical analysis in the North Anatolian Fault Zone (NAFZ) on the northern part of Suşehri Town, Turkey, Nat. Hazards, 92, 133-154, https://doi.org/10.1007/s11069-018-3195-1, 2018.

Demirağ, O.: Jeofizik yöntemlerle heyelan araştırmaları, TMMOB-JFMO (The Chamber of Geophysical Engineers of Turkish) publications, Jeofizik, 5(1); 43-50, Ankara, Turkey, 1991 (in Turkish).

Demirel, M., Tatar, O., Koçbulut, F.: Kinematics of the faults around the Koyulhisar (Sivas) region on the North Anatolian Fault Zone, Geol. Bull., Turkey, 59(3),357-370, 2016 (in Turkish).

Duman, T. Y., Nefeslioğlu, H., Gökçeoğlu, C., Sönmez, H.: 17/03/2005 Kuzulu (Sivas-Koyulhisar) heyelanı, Maden Tetkik ve Arama Genel Müdürlüğü Jeoloji Etütleri Dairesi, Hacettepe Üniversitesi, 2005.

Gren, A., Gross, R., Holliger, K., Horstmeyer, H., Baldwin, J.: Results of 3D georadar surveying and trenching the San Andreas fault near its northern landward limit, Tectonophysics, 368, 7-23, doi:10.1016/S0040-1951(03)00147-1, 2003.

Gökçeoğlu, C., Nefeslioğlu, H. A., Sönmez, H., Duman, T., Can, T.: The 17 March 2005 Kuzulu landslide (Sivas, Turkey) and landslide-susceptibility map of its near vicinity, Eng. Geol., 81 (1), 65-83, DOI:10.1007/s00254-006-0322-1, 2005b.

Göktürkler, G., Baklaya, Ç., Erhan, Z.: Geophysical investigastion of landslide: The Altındağ landslide site, Izmir (western Turkey), J. Appl. Geophys., 65, 84-96, https://doi.org/10.1016/j.jappgeo.2008.05.008, 2008.

Hack, R.: Geophysics for slope stability, Surv. Geophys., 21, 423-338, 2000.

Harrari, Z.: Ground penetrating radar (GPR) for imaging stratigrafic features and groundwater in sand dunes, J. Appl. Geophys., 36, 43-52, https://doi.org/10.1016/S0926-9851(96)00031-6, 1996.

Hastaoğlu, K. O.: Investigation of the groundwater effect on slow-motion landslides by using dynamic Kalman filtering method with GPS: Koyulhisar town center, Turkish J. Earth Sci., 1033-1046. DOI: 10.3906/yer-1210-10, 2013.

Hastaoglu, K. O.: Comparing the results of PSInSAR and GNSS on slow motion landslides, Koyulhisar, Turkey, Geomatics, Nat. Hazards and Risk, 7, 2, 786-803, DOI: 10.1080/19475705.2014.978822, 2016.

Hastaoğlu, K. O., Şanlı, D. U.: Monitoring Koyulhisar landslide using rapid static GPS: a strategy to remove biases from vertical velocities, Nat. Hazards, 58, 1275-1294, DOI:10.1007/s11069-011-9728-5, 2011.

Hastaoğlu, K. Ö., Türk, T., Koçbulut, F., Balık Şanlı, F., Poyraz, F.: "GNSS ve PS-InSAR Yöntemleri Kullanılarak Heyelanların İzlenmesi ve Afet Bilgi Sistemi Tabanlı Risk Analizlerinin Gerçekleştirilmesi: Koyulhisar (Sivas) Heyelanları" Final Report, TÜBİTAK Proje Number: 111Y111, www.tubitak.gov.tr, Turkey, 2015 (unpublished).

Hatiboğlu, O.: Investigation Of Koyulhisar (Sivas) Settlement Area In Terms of Slope Instability, Middle East Technical University, MS Thesis, Ankara, Turkey, 2009.

Hu, Z., Shan, W.: Landslide investigations in the northwest section of the lesser Khingan range in China using combined HDR and GPR methods, Bull. Eng.. Geol. Environ., 75, 591-603, DOI 10.1007/s10064-015-0805-y, 2016.

Lissak, C., Maquaire, O., Malet J.P., Lavigne, F., Virmoux, C., Gomez, C., Davidson, R.: Ground-penetrating radar observations for estimating the vertical displacement of rotational landslides, Nat. Hazards Earth Syst. Sci., 15, 1399-1406, doi:10.5194/nhess-15-1399-2015, 2015.

McCann, D. M., Forster, A.: Reconnaissance geophysical methods in landslide investigations, Eng Geol 29(1):59-78, https://doi.org/10.1016/0013-7952(90)90082-C, 1990.

MGM: Meteoroloji Genel Müdürlüğü (Turkish State Meteorological Service), Ankara Meteoroloji Bölge Müdürlüğü'nün Hidrotermal Şube Müdürlüğü (Hydrothermal Directorate of Ankara Meteorology Regional Directorate). https://www.mgm.gov.tr/ (accepted: 12.11.2008), 2016.

MTA: General Directorate of the Mineral Research and Exploration (MTA), (last access: 11.04.2018), http://yerbilimleri.mta.gov.tr/anasayfa.aspx, 2018.

Otto, J. C., Sass, O.: Comparing geophysical methods for talus slope investigations in the Turtmann valley (Swiss Alps), Geomorphology, 76, 257-272, doi:10.1016/j.geomorph.2005.11.008, 2006.

Över, D.: The Research of The landslide area ground of Koyulhisar district in Sivas with geophysical methods, Cumhuriyet University, MS Thesis, Sivas, Turkey, 2015.

Perrone, A., Iannuzzi, A., Lapenna, V., Lorenzo, P., Piscitelli, S., Rizzo, E., Sdao, F.: High-resolution electrical imaging of the Varco d'Izzo earthflow (southern Italy), J. Appl. Geophys., 56, 17-29, DOI:10.1016/j.jappgeo.2004.03.004, 2004.

Popescu, M., Şerban, R. D., Urdea, P., Onaca, A.: Conventional geophysical surveys for landslide investigations: Two case studies from Romania, Carpathian J. Earth and Environ. Sci., 11(1), 281-292, 2016.

Ristić, A., Abolmasov, B., Govedarica, M., Petrovački, D.: Shallow-Landslide Spatial Structure Interpretation Using A Multi-Geophysical Approach, Acta Geotechnica Slovenica, 47-59, 2012.

Sendir, H., Yılmaz, I.: Koyulhisar Heyelanlarına Yapısal ve Jeomorfolojik Açıdan Bakış, Cumhuriyet Üniversitesi Mühendislik Fakültesi Dergisi, Seri A: Yer Bilimleri, 18 (1), 47-54, 2001 (in Turkish).

Sendir, H., Yılmaz, I.: Structural, geomorphological and geomechanical aspects of the Koyulhisar landslides in the North Anatolian Fault Zone (Sivas, Turkey), Environ. Geol., 42, 52-60, https://doi.org/10.1007/s00254-002-0528-9, 2002.

Slater, L., Niemi, T. M.: Ground penetrating radar investigation of active faults along the Dead Sea transform and implications for seismic hazards within the city of Aqaba, Jordan, Tectonopyhsics, 368, 33-50, 2003.

Su, L., Xu, X., Geng, X., Liang, S.: An integrated geophysical approach for investigating hydro-geological characteristics of a debris landslide in the Wenchuan earthquake area, Eng. Geol., http://dx.doi.org/10.1016/j.enggeo.2016.11.020, 2016.

Tatar, O., Gürsoy, H., Gökçeoğlu, C., Koçbulut, F., Duman, T. Y., Kök S., Süllü, H., Şenyurt, A., İleri, N.: 17 Mart 2005 Sivas İli Koyulhisar İlçesi Sugözü Köyü Kuzulu Mahallesi Heyelanı 2. Değerlendirme Raporu, http://www.koyulhisar.gov.tr/bulten3.doc., 2005 (in Turkish).

Tatar, O., Gürsoy, H., Altunel, E., Akyüz, S., Topal, T., Sezen , T. F., Koçbulut, F., Mesci, L., Kavak, K.Ş., Dikmen, Ü., Türk, T., Poyraz, F., Hastaoğlu, K., Ayazlı, E., Gürsoy, Ö., Polat, A., Akın, M., Demir, G., Zabcı, C., Karabacak, V., Çakır, Z.: Kuzey Anadolu Fay Zonu üzerinde Kelkit Vadisi boyunca yer alan yerleşim alanlarının doğal afet risk analizi, CBS tabanlı afet bilgi sistemi (KABİS) tasarımı: Proje tanıtımı ve ön bulgular. Aktif Tektonik Araştırma Grubu 11. Çalıştayı, TÜBİTAK-MAM Yer ve Deniz Bilimleri Enstitüsü Gebze-Kocaeli, Türkiye, 14-16, 2007 (in Turkish).

Terlemez, İ., Yılmaz A.: Ünye-Ordu-Koyulhisar-Reşadiye arasında kalan yörenin stratigrafisi, TJK Bülteni, 21, 179-191, 1980 (in Turkish).

Timothy, R. H., Davies, Warburton J., Stuart A. Dunning, Alodie, Bubeck, A. P.: A large landslide event in a post-glacial landscape: rethinking glacial legacy, Earth Surface Processes and Landforms, 38(11), 1261-1268, https://doi.org/10.1002/esp.3377, 2013.

Topal, T., Hatiboğlu, O.: Assessment of slope stability and monitoring of a landslide in the Koyulhisar settlement area (Sivas, Turkey), Environ. Earth Sci., 74(5), DOI 10.1007/s12665-015-4476-6, 2015.

Toprak, G. M. V.: Tectonic and stratigraphic characterstics of the Koyulhisar segment of the North Anatolian Fault Zone (Sivas-Turkey), METU (unpublished), PhD. Thesis, Ankara, Turkey, 121, 1989.

Türk, T.: Hava fotoğrafı ve optik uydu görüntüleri yardımıyla yatay yer değiştirmelerin belirlenmesi, Havacılık ve Uzay Tekn. Derg., 6 (1), 71-79, 2013 (in Turkish).

UDİM: Ulusal Deprem İzleme Merkezi (National earthquake monitoring center), Boğaziçi Universty KOERI (Kandilli Observatory And Earthquake Research Institute), www.koeri.boun.edu.tr/sismo/, (last access: 11.04.2018), Istanbul, Turkey, 2016.

Uysal, S.: Koyulhisar (Sivas) yöresinin jeolojisi, General Directorate of the Mineral Research and Exploration (MTA) Report number: 9838, 1995 (in Turkish).

Ulusay, R., Aydan, Ö., Kılıç, R.: Geotechnical assessment of the 2005 Kuzulu landslide (Turkey), Eng. Geol., 89(1-2), 112-128, 2007.

Wilchek, L.: Ground Penetrating Radar for Detection of Rock Stucture, MS Thesis, Alberta University, Canada, 2000.

Yılmaz, I.: A case study from Koyulhisar (Sivas-Turkey) for landslide susceptibility mapping by artificial neural Networks, Bull. Eng. Geol. and the Environ., 68, 297-306, 2009.

Yılmaz, I., Ekemen T., Yıldırım, M., Keskin İ., Özdemir, G.: Failure and flow development of a collapse induced complex landslide: the 2005 Kuzulu (Koyulhisar, Turkey) landslide hazard, Environ. Geol., 49, 467-476, 2005.

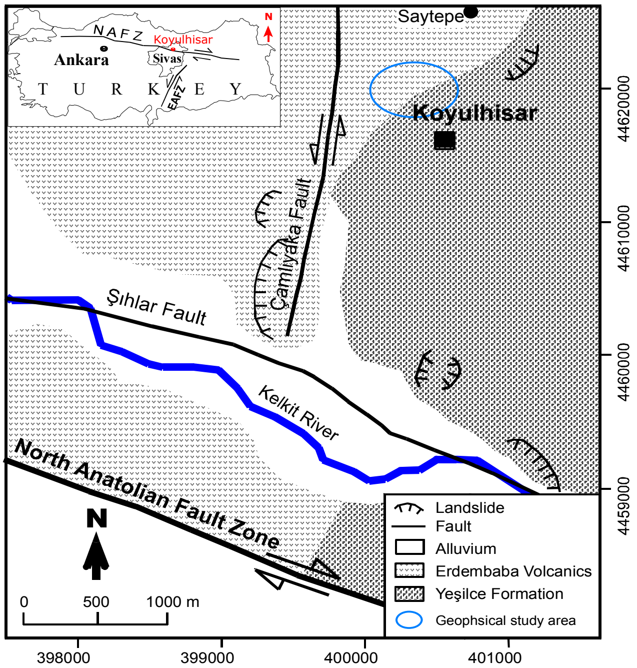

Figure 1. Geological map of study area arranged from Sendir and Yılmaz (2002) and Hastaoğlu (2016).

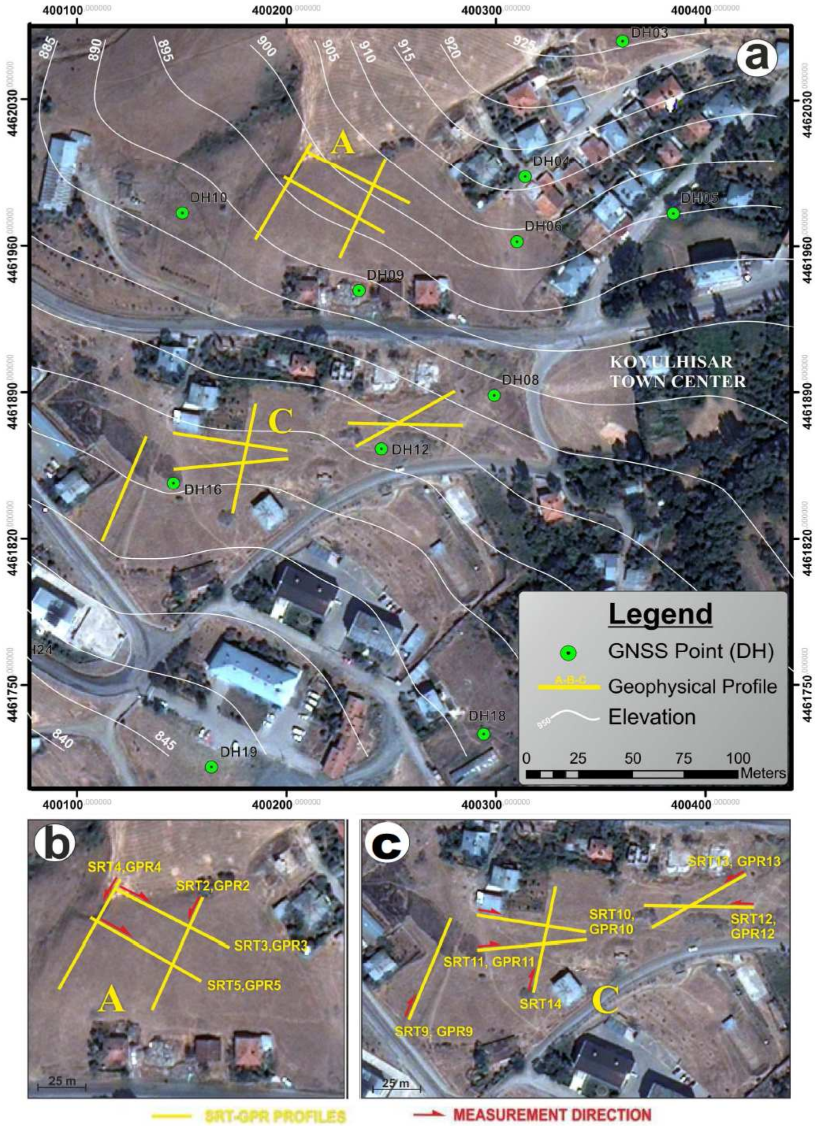

Figure 2. (a) Geophysics and geodetic data collection locations in the study area. (b), (c) and (d) geophysics profile details.

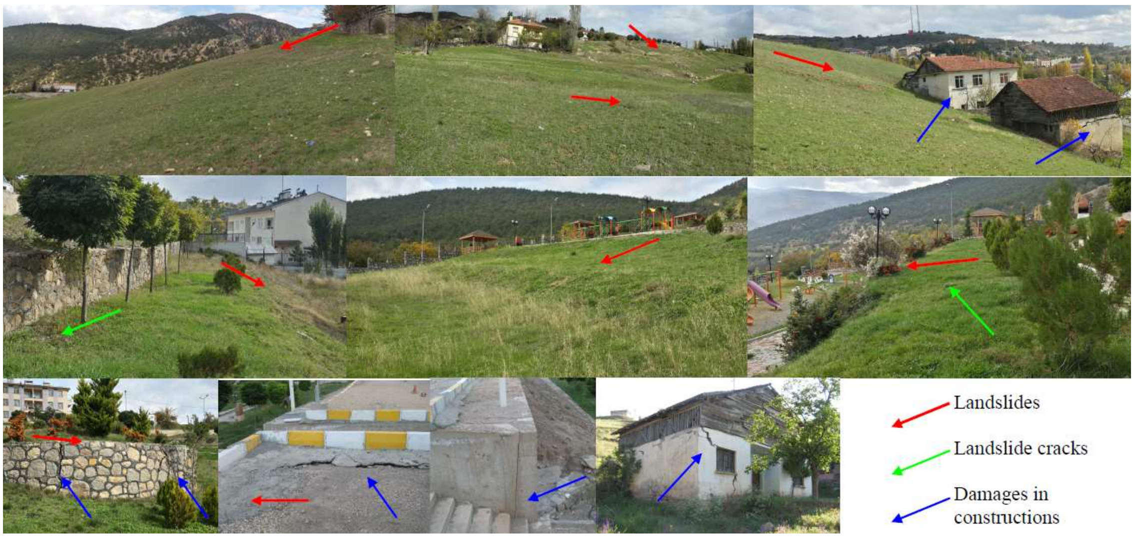

Figure 3. Landslide scene photos (landslide, lanslide cracks and constructional damages).

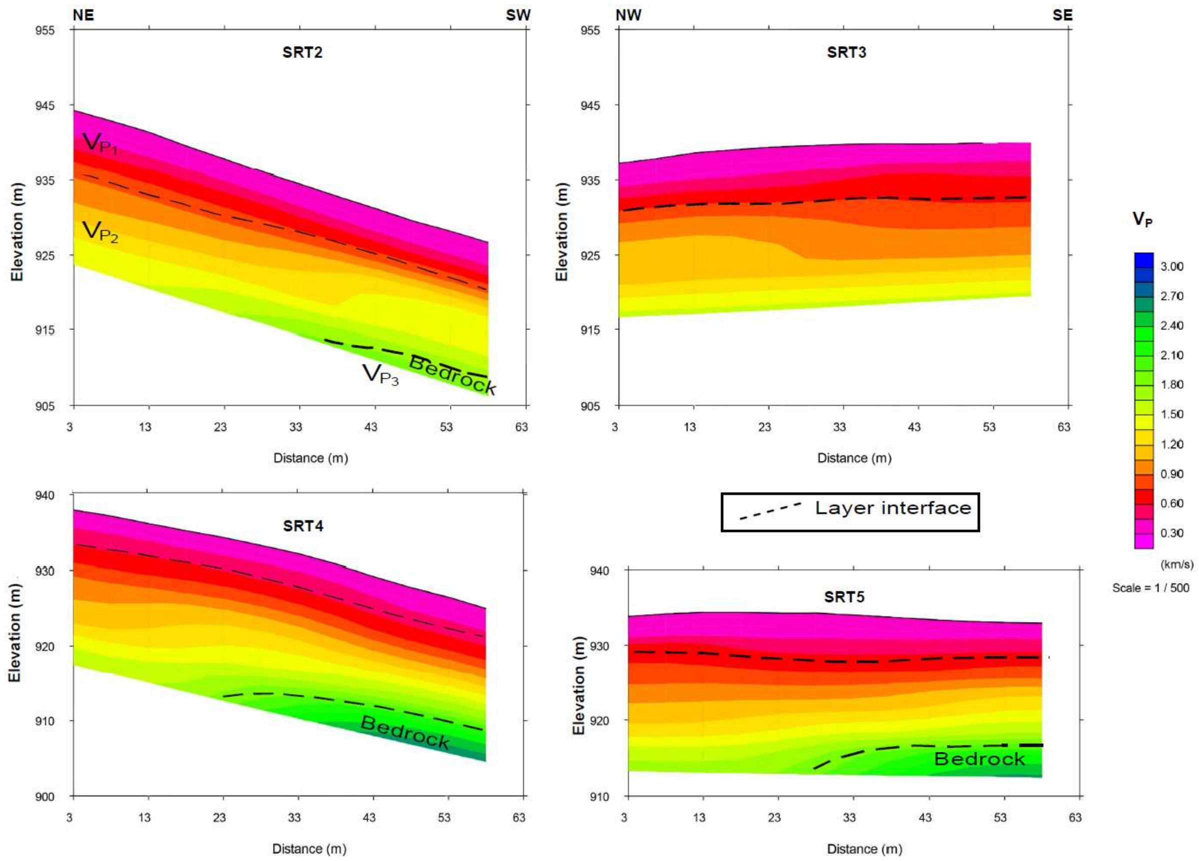

Figure 4. The seismic profiles of the area **A**. The uppermost boundary of the bedrock layer (V_{P3}) on the SRT images is aproximately GPR depth. The lower seismic velocity loose layers (consisting of soil and alluviums, the average seismic V_{P1}=0.3 km/s and V_{P2}=1.0 km/s) are on the bedrock (the average seismic V_{P3}>2.0 km/s).

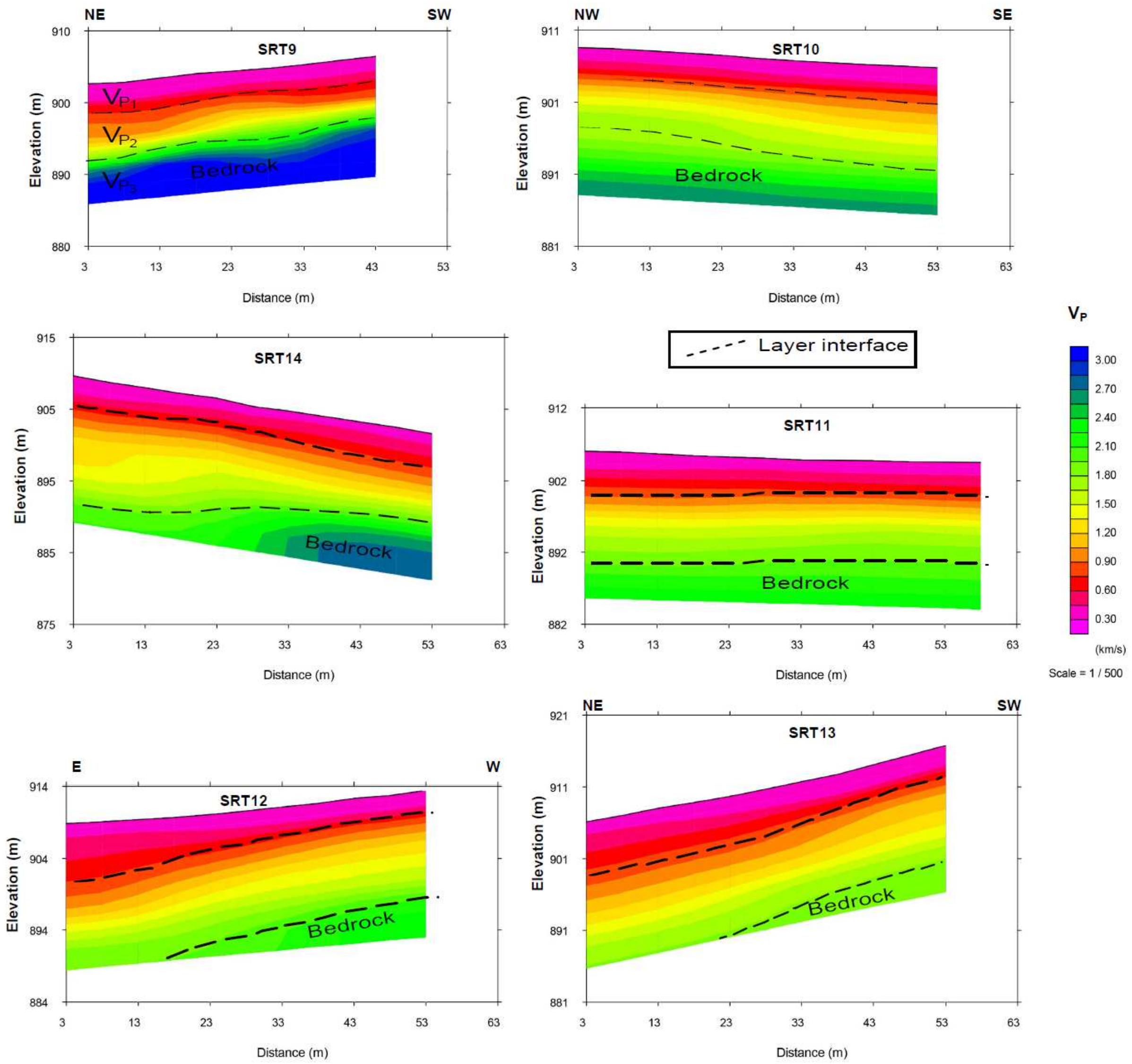

Figure 5. The sismic profiles of the area **C**. The uppermost boundary of the bedrock layer (V_{P3}) on the SRT images is aproximately GPR depth. The lower seismic velocity loose layers (consisting of soil and alluviums, the average seismic V_{P1}=0.3 km/s and V_{P2}=1.0 km/s) are on the bedrock (the average seismic V_{P3}>2.0 km/s).

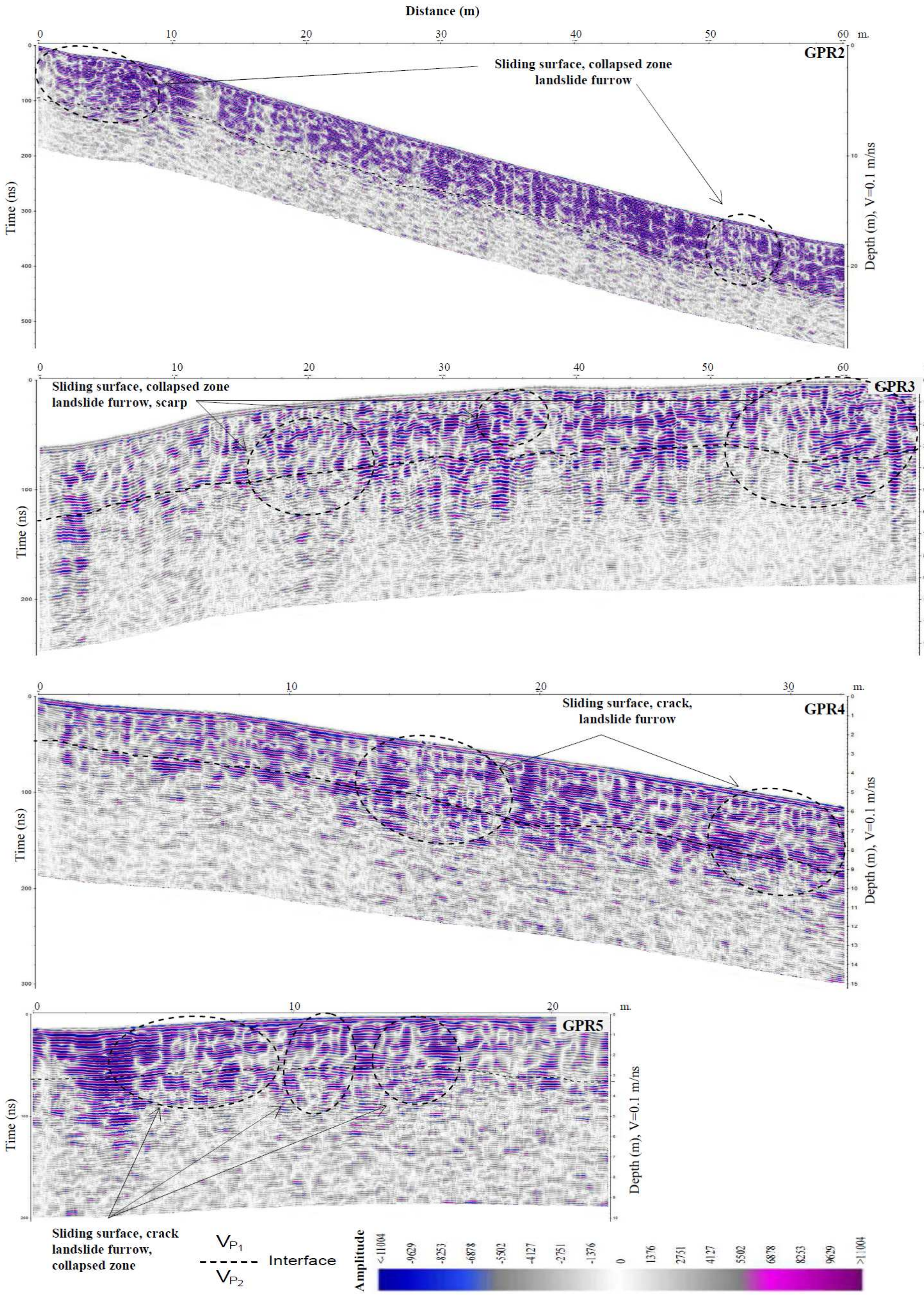

Figure 6. GPR profiles in A area and the deformations in the loose layers (the seismic V_{P1} and V_{P2} layers).

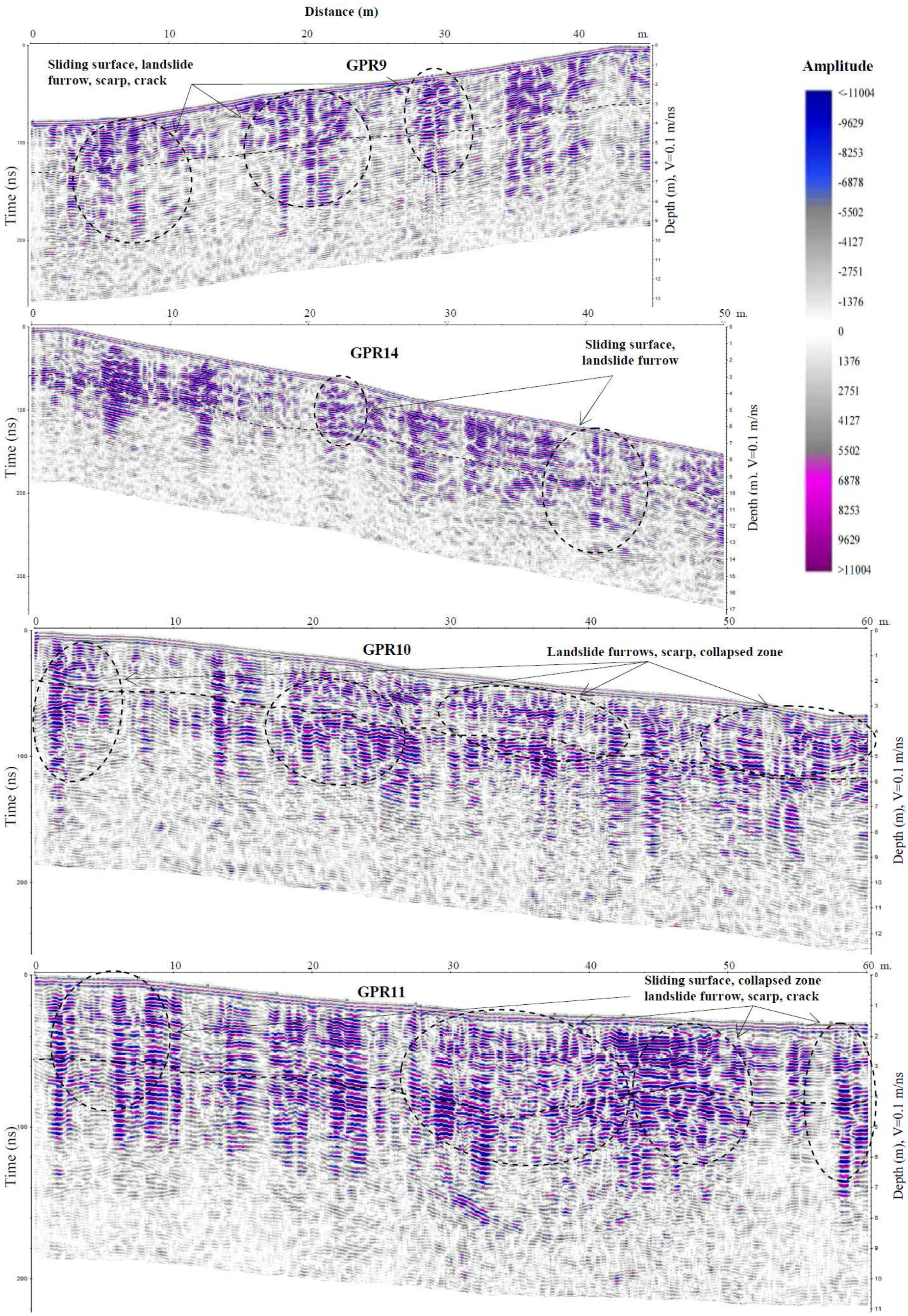

Figure 7. GPR profiles in the C-west area and the deformations in the loose layers (the seismic V_{P1} and V_{P2} layers).

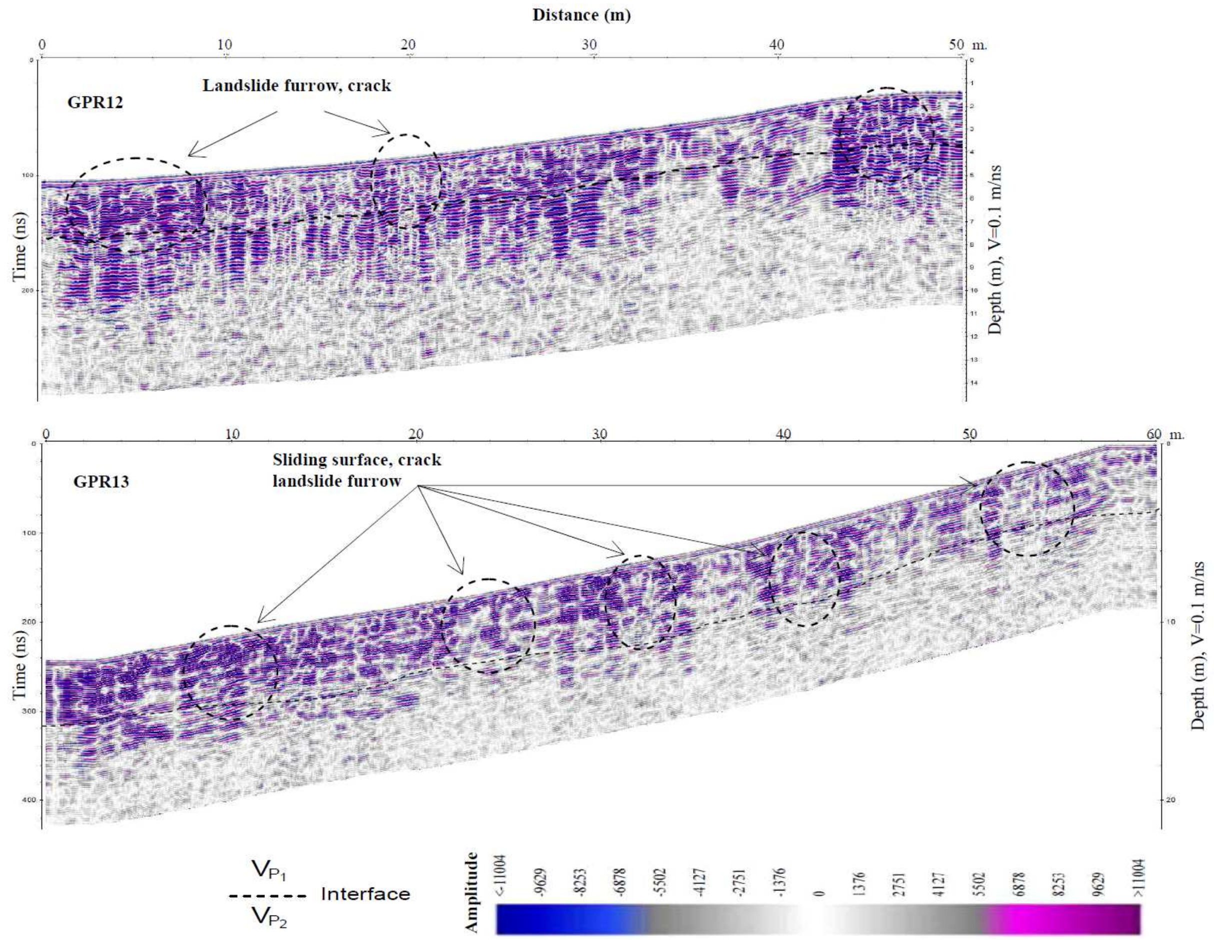

Figure 7. (…contiune) GPR profiles in the C-east area and the deformations in the loose layers (the seismic V_{P1} and V_{P2} layers).

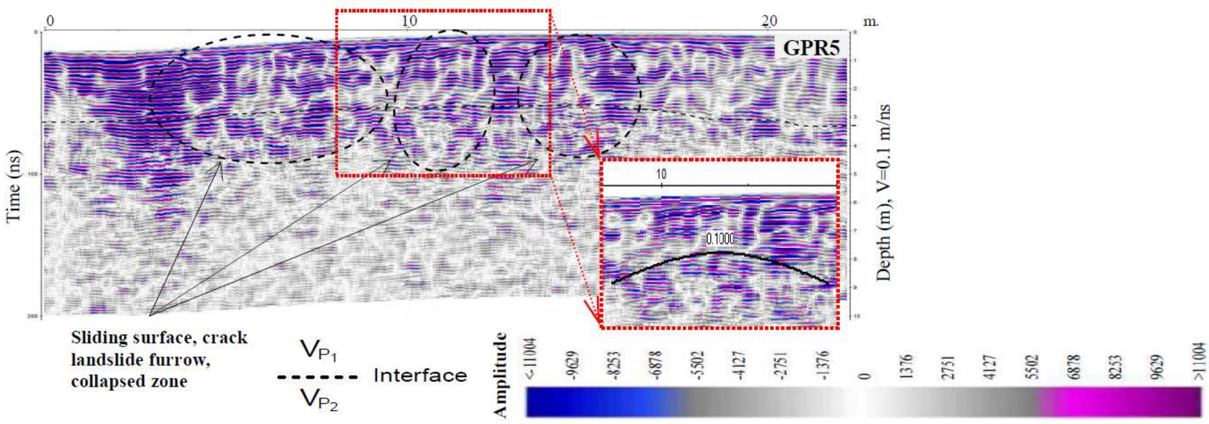

Figure 8. EM wave velocity calculated for reflection surface in GPR5 in the C-east area cross section as representing all the GPR profiles.

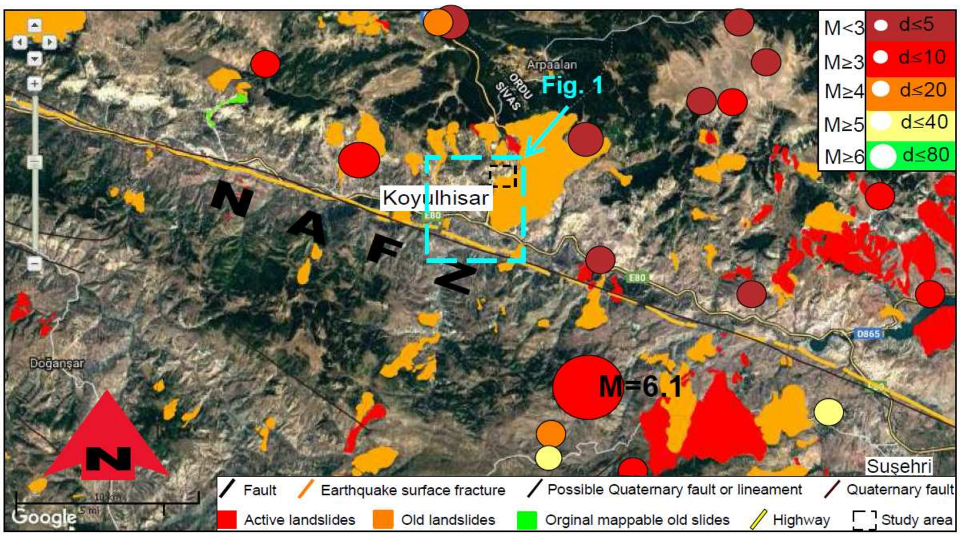

Figure 9. Seismic activity of the study area and its surroundings by the data between 1900-2015 and the landslide areas (UDIM, 2016; MTA, 2018).

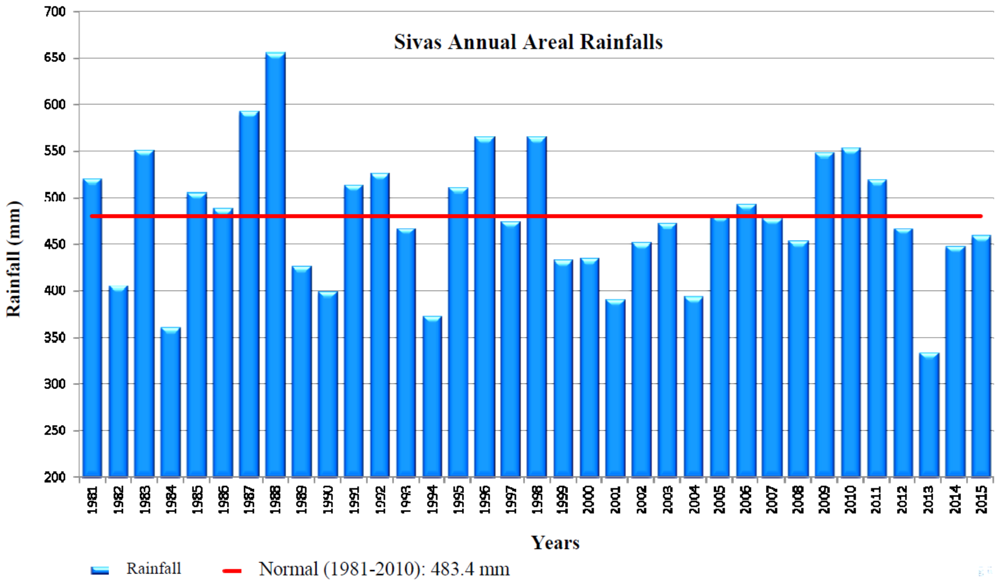

Figure 10. Precipitation distribution in between 1981-2015 years of Sivas (MGM, 2016).

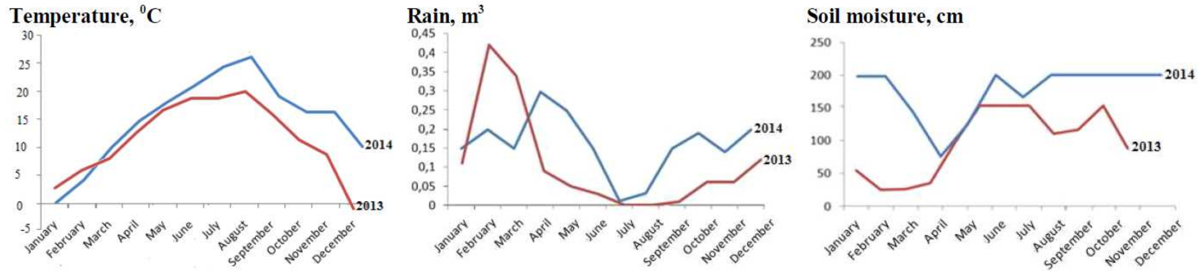

Figure 11. Average monthly temperature (T, ^{0}C), rainfall (m^3) and soil moisture content (cm) change graphics of the study area and its surrounding for 2013-2014. It was prepared from the project data (Hastaoğlu et al., 2015).

Table

Table 1. The annual average meteorological values of Sivas by years between 1950-2015 (MGM, 2016).

SIVAS	January	February	March	April	May	June	July	August	September	October	November	December
The average tempreture (^{0}C)	-3.2	-2.0	2.9	9.1	13.5	17.2	20.2	20.2	16.2	10.8	4.6	-0.6
The average the highest tempreture (^{0}C)	1.0	2.6	8.1	15.3	20.0	24.0	27.9	28.5	24.7	18.4	10.6	3.7
The average the lowest tempreture (^{0}C)	-7.0	-6.2	-1.7	3.4	7.2	9.9	12.0	11.9	8.3	4.4	-0.2	-4.2
The average sunshine duration (hour)	2.3	3.3	4.5	6.2	8.1	10.4	12.1	11.4	9.4	6.3	4.1	2.3
The average number of rainy days	13.0	12.4	13.7	14.0	14.4	8.8	2.5	2.1	4.3	8.0	9.5	12.1
The average monthly total rainfall (kg/m^2)	42.0	40.3	46.0	59.1	60.7	34.8	8.5	5.9	16.9	32.9	41.0	44.2
The highest and the lowest values occurring over many years (1950-2015)												
The highest tempreture (^{0}C)	14.6	18.1	25.2	29.0	32.0	35.5	40.0	39.4	35.7	30.5	22.8	19.4
The lowest tempreture (^{0}C)	**-34.6**	**-34.4**	**-27.6**	**-10.9**	**-4.2**	**-0.3**	**3.4**	**3.2**	**-3.8**	**-8.1**	**-24.4**	**-27.0**
Daily total the highest rainfall	**2 May 1991**	**55.0 kg/m^2**	Daily the fastest wind			**5 Jan. 1996**		**122.8 km/h**	**The highest snow**		**2 Feb. 1950**	**110.0 cm**